Carbohydrate Research 542 (2024) 109190

Contents lists available at ScienceDirect

Carbohydrate Research

journal homepage: www.elsevier.com/locate/carres

Effect of Fenton reaction parameters on the structure and properties of oxidized wheat starch

Adrien Letoffe [a,*], Reza Hosseinpourpia [b,c], Valentin Silveira [a], Stergios Adamopoulos [a]

[a] Department of Forest Biomaterials and Technology, Swedish University of Agricultural Sciences, Vallvägen 9C, 75007, Uppsala, Sweden
[b] Department of Forestry and Wood Technology, Linnaeus University, Lückligs Plats 1, 35195, Växjö, Sweden
[c] College of Forest Resources and Environmental Science, Michigan Technological University, Houghton, MI, 49931, United States

ARTICLE INFO

Keywords:
Starch oxidation
Hydrogen peroxide
Metal catalyst
Granule morphology
Amylose content

ABSTRACT

Wheat starch was oxidized through a Fenton reaction by hydrogen peroxide and Iron II sulfate as a catalyst at various concentrations and reaction duration. The formation of carbonyl and carboxyl groups confirmed the starch oxidation as determined with Fourier-transform infrared (FTIR) spectroscopy. The degree of oxidation was estimated by carbonyl and carboxyl titration. The various oxidized wheat starches presented considerable variations in their oxidation level as a function of the catalyst concentration and oxidative process duration. The effect of the Fenton reaction parameters on the starch macromolecular chains and microstructure was evaluated by X-ray diffraction and amylose content estimation. Significant depolymerization of the starch macromolecules was observed, mainly in the starch amorphous phase, followed by a degradation of the crystalline phase at a higher oxidation level. SEM observations revealed changes in starch structure, which ranged from minor degradation of the starch granules to a more crosslinked morphology.

1. Introduction

The interest in using bio-based resources to produce materials and replace petroleum-derived products has grown in the last few decades. Developing environmentally friendly and cost-effective processes is centred on this approach and requires constant improvement. Different natural polymers, such as lignin, proteins, tannins, and polysaccharides, are widely used today for material development. Starch, one of the most abundant polysaccharides on earth, is the main component of cereals, roots, and tubers. It naturally exists in a granule shape in the plant and comprises of two structurally distinct α-d-glucan components, linear amylose and branched amylopectin [1,2]. Starch is commonly used in various applications, including paper, textile, and food industries [3–6], or form a biopolymer basis for the production of hydrogels [7] and adhesive formulations [8–10].

Today, starch is of great interest to the wood industry as an adhesive component [8–10] due to its high availability, medium to low cost, and potential to easily tailor its properties [3,8–13]. However, applying starch in its native form in wood adhesives presents several limitations, which are related to its hydrophilic structure, high viscosity, and low reactivity. Starch properties are traditionally altered through various modification techniques, such as chemical, mechanical, thermal, and enzymatic modification. Chemical modification of starch is a well-established approach that aims to substitute at least one of the hydroxyl groups in the glucose units of starch via cross-linking, acid hydrolysis, oxidation, etherification, esterification, and ionic reactions, or grafting with other polymers [12–14]. The chemically modified starch can be used solely or with other polymers [8,13]. A common chemical modification method of starch is oxidation, which occurs by reacting starch with an oxidizing agent under controlled reaction conditions, e.g. temperature and/or pH. The oxidation reaction of starch is generally carried out by initial carbonylation or carboxylation of C2, C3 and C6 atoms in the glucose units and then cleavage of α-(1 → 4)-glucosidic linkages [15]. The content of carbonyl and carboxyl groups in oxidized starch is used to determine the degree of starch oxidation. Besides the origin and amylose and amylopectin ratio of starch, the final properties of oxidized starch highly depend on the oxidizing agent and the reaction conditions.

The most frequently used starch oxidizing agents in the industry are sodium hypochlorite, sodium periodate and hydrogen peroxide [15–18]. Sodium hypochlorite has been one of the oldest and most popular commercially used oxidants due to its chemical efficiency [19]. However, it is of limited use because of its high price and environmental pollution issues since the oxidation reaction produces a toxic chlorinated

* Corresponding author.
E-mail address: adrien.letoffe@slu.se (A. Letoffe).

https://doi.org/10.1016/j.carres.2024.109190
Received 19 March 2024; Received in revised form 11 June 2024; Accepted 13 June 2024
Available online 15 June 2024

by-product [15–18]. Starch oxidation by sodium periodate is carried out by cleavage of C2 and C3 bonds in the glucose units, which forms a highly reactive dialdehyde starch. Similarly, major drawbacks have to do with the high cost of sodium periodate and the production of toxic by-products. At the same time, another disadvantage is the significant impact on starch morphology, i.e. it causes degradation of starch granules [16–18].

Unlike other oxidizing agents, hydrogen peroxide is of low cost and creates no harmful by-products as it decomposes into hydrogen ions, radicals and water. Therefore, starch oxidation by hydrogen peroxide is one of the most preferable methods [20,21]. However, due to the low reactivity of hydrogen peroxide leading to long reaction times, the oxidation process requires the presence of a catalyst, mostly a metal catalyst, while the presence of UV light or high frequency has also been studied [22,23]. High temperature or high pH are additional requirements. The reaction of hydrogen peroxide in presence of a metal catalyst is called Fenton reaction. The metal catalyst, such as Iron (II), is oxidized by hydrogen peroxide, forming a hydroxyl radical and a hydroxide ion in the process. Iron (III) is then reduced back to Iron (II), forming a hydroperoxyl radical and a proton. As such, the reaction creates two different oxygen-radical species, which can be used to oxidize organic maters.

Starch oxidation by hydrogen peroxide in the presence of an iron catalyst, provides a homogeneous reaction ambient involving catalytic production of the hydroxyl radicals by reduction of hydrogen peroxide by ferrous iron [24]. The reaction also includes rate-limiting reduction equilibrium of ferrous cation to ferric iron. Like the sodium hypochlorite method, the oxidized starch obtained through the Fenton reaction also contains aldehyde and carboxyl groups. The degree of oxidation and the properties of modified starch are mainly controlled by adjusting the reaction conditions, e.g. temperature, pH, and reagent and catalyst concentrations [4,15,25,26].

As explained previously, oxidation comes with a cleavage of α-(1 → 4)-glucosidic linkages, which decreases the macromolecular length and starch viscosity and degradation of starch granules. When the reaction is extend enough, it can lead to the degradation of the starch macromolecule into smaller molecules, such as alcohols, aldehydes, ketones or carboxylic acids, or in carbon dioxide and water. All these changes in the physicochemical properties and morphology of starch affect its functional and binding qualities, which are particularly relevant for use as a wood adhesive component. The impact of macromolecular degradation on a polymer's mechanical performance is well known in the polymer field, where a macromolecule cleavage reaction can imply a complete switch of mechanical behaviour from ductile to brittle [27,28]. Accordingly, optimum starch oxidation would ensure the highest possible oxidation degree and minimal granules' degradation. A higher rate of carbonyl and carboxyl groups in oxidized starch should impart higher reactivity for participation in useful reactions for wood adhesives, such as cross-linking [29]. However, information on the structure-property relationships of oxidized starch is quite limited [30]. This study aimed to elucidate the effect of Fenton reaction conditions, precisely process duration and catalyst level, on the physical, chemical and thermal properties of oxidized starch, and morphology (shape, surface features) of starch granules.

2. Materials and methods

2.1. Materials

Native wheat starch was kindly provided by Lantmännen (>95 %, Stockholm, Sweden). The metal catalyst used for the Fenton reaction was Iron II sulfate (ACS reagent, ≥99.0 %, Sigma-Aldrich). The oxidizing agent, hydrogen peroxide (H_2O_2), was used as a 30 wt % solution (Sigma-Aldrich). Ethanol (≥99.5 %) was supplied by VWR (Stockholm, Sweden), while phenolphthalein indicator (0.5 wt %), sodium hydroxide (NaOH, ≥98 %), acetone (≥99 %), and hydrochloric acid were purchased from Sigma-Aldrich (Stockholm, Sweden).

2.2. Starch oxidation

5 g of vacuum oven-dried native wheat starch (40 °C overnight) was dispersed in a 250 ml three-neck round bottom flask containing 100 ml of distilled water at 35 °C for 10 min using magnetic stirring. Iron II sulfate (pre-dissolved in 10 ml water) was added to the starch dispersion at concentrations of 0.1, 0.2, 0.3, 0.4, 0.5 and 1 % $wt/wt_{dried\ starch}$). After stirring for 10 min, the Fenton reaction was initiated by adding H_2O_2 to the mixture at an H_2O_2:glucose group molar ratio of 2:1. The solution pH was not controlled. The stirring was maintained at 35 °C for a growing duration from 1 to 8 h or until a significant sample mass loss was observed. The oxidation of starch was halted by adding 10 ml of acetone to the solution. The oxidized wheat starch (OWS) samples were then purified by three times washing with distilled water by replacing the supernatant with fresh water after each centrifugation. Subsequently, the OWSs were washed, centrifuged with ethanol and dried in a vacuum oven at 40 °C and 0.3 bar for 24 h. Finally, the final product weight was determined.

2.3. Fourier-transform infrared (FITR) spectroscopy

The FTIR spectroscopy analysis was performed using an Alpha FTIR spectrometer-Bruker with a versatile high throughput ZnSe ATR crystal (Karlsruhe, Germany), in a wavelength region from 4000 to 550 cm^{-1}, accumulating 32 scans with a resolution of 4 cm^{-1}.

2.4. Carbonyl and carboxyl titration

The carbonyl content was evaluated using the titration method. 0.2 g of starch was gelatinized in water before being cooled down to 40 °C. The pH was adjusted to 3.2 with 0.1 M HCl solution before adding 15 mL of hydroxylamine reagent. The solution was stirred for 4 h at 40 °C. The excess hydroxylamine was rapidly titrated at pH 3.2 by 0.1 M HCl solution. A blank test was also performed. The hydroxylamine reagent was prepared by dissolving 25 g of hydroxylamine hydrochloride in 100 mL of 0.5 M NaOH solution. The solution's final volume was then adjusted to 500 mL with distilled water. The carbonyl content was estimated as:

$$Carbonyl\ content = \frac{(V_{blank} - V_{sample}) * C_{HCl} * 0,028}{m} * 100$$

With V_{blank} and V_{sample} the HCl volume used for the blank test and the sample titration respectively, C_{HCl} the acid solution molarity, and m the sample mass.

The carboxyl content was also measured by titration. 0.2 g of starch was gelatinized in water until complete dissolution with a few drops of phenolphthalein indicator. The solution was titrated with NaOH solution at 0.1 M until colouration. A blank test was also performed. The carboxyl content was estimated has:

$$Carboxyl\ content = \frac{(V_{sample} - V_{blank}) * C_{NaOH}}{m/M} * 100$$

With V_{blank} and V_{sample} the NaOH volume used for the blank test and the sample titration respectively, C_{NaOH} the acid solution molarity, m the sample mass, and M the molar mass of the starch glucosides groups.

2.5. Amylose content

The amylose content of the starch samples, before and after oxidation, was determined by the iodine colorimetric method with an ultraviolet–visible spectrophotometer (Lambda 35 UV/VIS spectrometer, PerkinElmer, city, country) [31,32]. The starch amylose content was evaluated by the absorbance peak at 620 nm and compared with the standard curve.

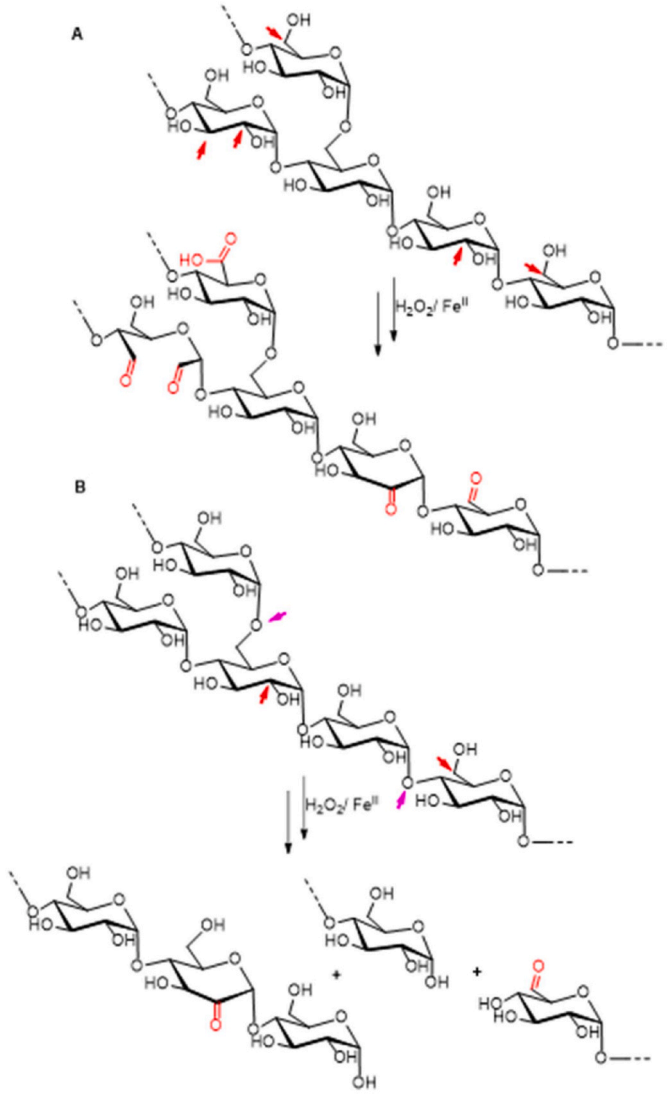

Fig. 1. Fenton oxidation mechanism: main oxidation features in oxidized starch (A), and characteristic oxidative degradation products (B). Red arrows show potential oxidation sites in starch whereas purple arrows show glyosidic bond cleavage sites.

2.6. X-ray diffraction (XRD)

The crystalline structure of OWSs was determined using an X-ray diffractometer (PANalytical Empyrean, Almelo, Netherlands) equipped with a Cu LFF HR X-ray tube, programmable anti-scatter slit, and a PIXcel3D detector. The Cu Kα radiation and a detector operating at 45 kV and 40 mA were used. The scanning degrees, i.e. 2θ range, was 5–60° with a scanning speed of 1°/min. The relative crystallinity of starch was calculated as the ratio of the area of the different crystalline diffraction peaks to the total area of the crystalline and amorphous region:

$$X_x = \frac{Crystalline\ peak\ area}{Total\ Area} \times 100$$

The positions and half-width in radians of the diffraction peaks can also be used to observed variation of the various crystalline dimension following the Fenton reaction.

2.7. Scanning electron microscopy (SEM)

The morphology of OWS granules was visualized using an Environmental Scanning Electron Microscope (PhilipsXL-30 ESEM, HITACHI, Japan) at 10 KV, with a spot size of 4.3 using the secondary electrons detector for a magnification of 200 and 1000. Before observation, the samples were coated with gold using a sputter coater (Emitech k550X, Quorum Emitech, England).

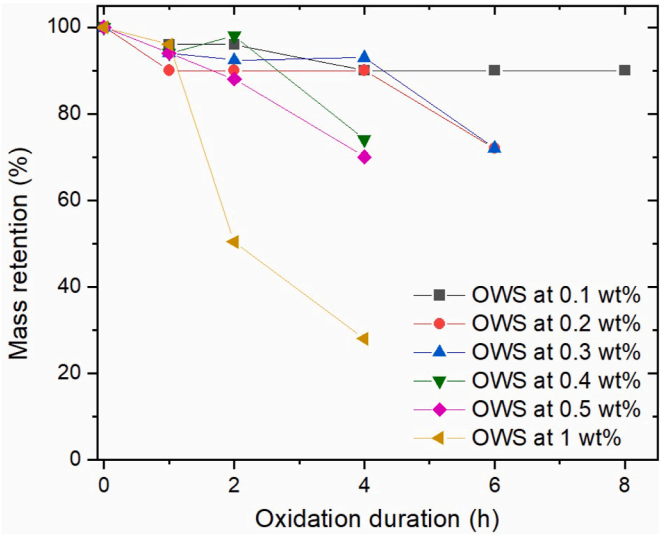

Fig. 2. Mass retention (%) after washing and drying of OWSs at different catalyst concentrations and oxidation duration.

2.8. Thermogravimetric analysis

Thermogravimetric analyses (TGA) of OWS samples were performed using a Mettler-Toledo TGA2 (Mettler Toledo, Switzerland), under nitrogen with a flow rate of 40 mL min^{-1}, with alumina pans. The samples were heated from 30 to 600 °C at a heating rate of 10 °C min^{-1}.

2.9. Water absorption capacity

0.1 g of each dry OWS was placed in a centrifuge tube containing 5 ml of distilled water, agitated to obtain the complete dispersion of starch in the water, and then centrifuged at 5000 rpm for 5 min. After removing the excess water, the tubes were weighed and the gain in weight was used to calculate percent gain as the water absorption capacity (WAC).

3. Results and discussion

3.1. Effect of reaction conditions on sample final weight

As mentioned before, the oxidation reaction also comes with a cleavage of α-1,4 glucosidic linkages that decreases the starch macromolecular length and causes degradation the starch granules. When the degradation is extend enough, starch macromolecules can be cut into small chains segment of a few glucose groups soluble in water, or into smaller molecules. In some of the stronger conditions, the end products can be carbon dioxide and water. Those small molecules can be lost during the cleaning step at the end of the oxidation process, which implied a notable mass reduction [4,14,15,25,26,33–35]. Fig. 1 presents the two possible pathways, the oxidation of the OWS macromolecules and their degradation.

Since the targeted application of OWS is wood adhesives, a high level of degradation and material loss must be avoided. As such, for each catalyst concentration, the reaction was performed in growing duration (with at least 1, 2 and 4 h duration) until a significant mass loss was observed or the maximum duration of 8 h was reached. To observe any mass decline following the Fenton reaction, the mass of each OWS was measured following the washing and drying process and compared to

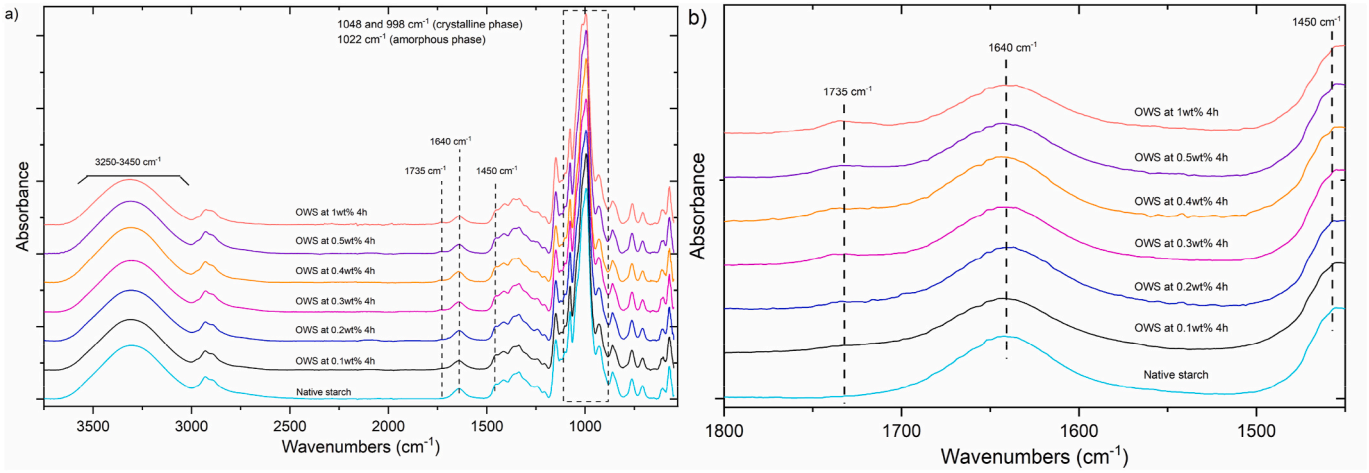

Fig. 3. FTIR spectra of native starch and OWSs prepared at different catalyst concentration at 4 h oxidation duration: spectra from 4000 to 550 cm^{-1} (a) and zoom on the 1450, 1640 and 1735 cm^{-1} bands (b).

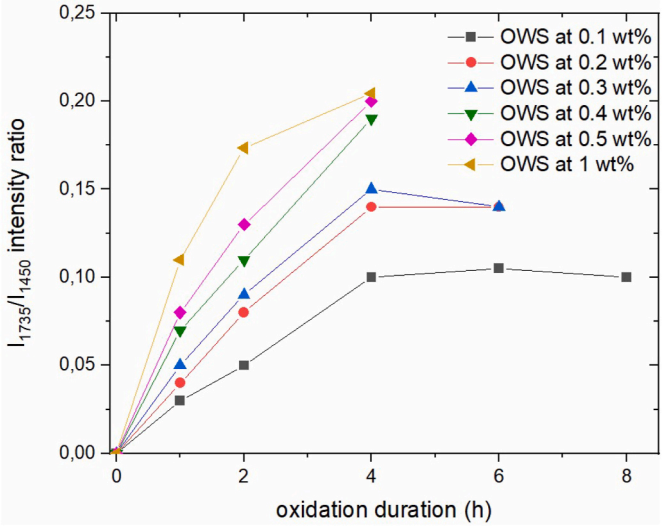

Fig. 4. Evolution of absorption intensity of the OWS bands at 1735 cm^{-1}(I_{1735}) normalized by the intensity of the 1450 cm^{-1} band intensity (I_{1450}) with different catalyst concentrations and oxidation duration.

the initial sample mass (5 g). The OWS mass retention is presented in Fig. 2, with any fall indicating a material loss due to oxidation. All OWSs had a minimal mass loss of 5–10 % after 1 h of treatment. The OWS prepared at the lowest catalyst concentration of 0.1 wt % presented a maximum mass loss of 10 % after 4 h of oxidation; no change was observed when the duration reached 6 and 8 h. However, the OWSs prepared with higher catalyst concentration presented a more significant mass loss following the oxidation duration; after 6 h for the OWSs prepared at 0.2 and 0.3 wt %, after 4 h for the OWSs prepared at 0.4 and 0.5 wt %, and after 2 h for the OWS prepared at 1 wt %.

The OWS mass loss was generally increased with increasing catalyst concentration, which should be due to the starch macromolecule degradation. The oxidation reaction primarily occurs on the –OH groups at the C-2, C-3 and C-6 positions but can also happen at the α-1,4 glucosidic linkages. This leads to depolymerization [4,15], debranching of the amylopectin [25,26,33,34], macromolecules chain cleavage [4,15,35], and, as explained earlier, scission of already oxidized chains. The correlation between the level of mass loss and the catalyst content can be explained by the higher rate of H_2O_2 decomposition in hydroxyl radicals, water and ions species and a much higher oxidation rate [36,37].

3.2. Effect of reaction conditions on the starch composition and chemical properties

3.2.1. FTIR spectra analysis

The chemical properties of OWSs were analyzed with FTIR spectroscopy, and carbonyl and carboxyl titration. Fig. 3 presents the FTIR spectra of the OWSs prepared at different catalyst levels for a process duration of 4 h. Those curves were selected to illustrate the evolution of oxidation conditions for a chosen duration. In contrast, the other OWSs' spectra are presented in Supporting Information (Figs. S1–S6). After applying a baseline, the spectra were normalized using the 1450 cm^{-1} band intensity associated with the C–H bending vibration [38].

The large band between 3450 and 3250 cm^{-1}, associated with the –OH groups stretching, was present on all OWS spectra, indicating that not all the starch –OH groups were consumed in the reaction. Fenton reactions resulted in a new absorption band at 1735 cm^{-1} on the modified starch polymers assigned to the C═O stretching vibration of the carbonyl and carboxyl groups [38,39]. The normalized intensities of this peak in different OWSs are shown in Fig. 4. For each catalyst concentration, the OWSs presented a steep rise of the 1735 cm^{-1} normalized intensity with increasing oxidation duration. After 4 h of treatment for all OWSs, a maximum was obtained, followed by stabilization for the OWSs prepared for 6 h. This trend showed a clear impact of catalyst concentration and Fenton reaction duration on the oxidation degree of OWSs. A process duration of 4 h and as low catalyst concentration as 0.4 wt % are sufficient for a maximum degree of starch oxidation.

Another band at 1640 cm^{-1} was present in all OWS spectra and is associated with the H_2O bending vibration [40]. This band comes from water molecules trapped in the starch structure due to the remaining –OH groups. No variation of this band intensity could be observed following the starch oxidation. Others have reported a significant variation of this band's intensity at high levels of starch oxidation [40,41].

The last significant part of the OWS spectra was a group of vibrational bands between 980 and 1100 cm^{-1}. Those bands are linked to the short-range structure and crystallinity of starch. Most works separated this part of the spectra between three bands linked to the starch backbones' C–O and C–C stretching vibrations. Those bands were determined to be very sensitive to the physical state of starch [42,43]. Two bands, at 1048 and 998 cm^{-1}, are assigned to the starch crystalline phase, and the 1022 cm^{-1} band is mainly assigned to the amorphous phase [33]. As such, variation of the starch microstructure would affect the proportion between those bands. Various intensity ratios were proposed using those bands to characterize the starch short-range structure, and the 1022:998

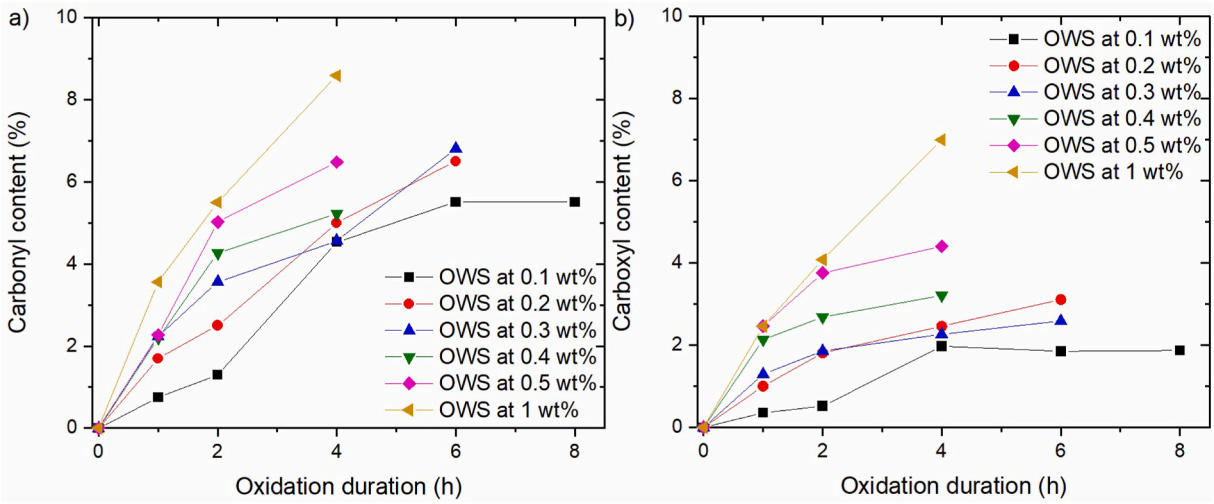

Fig. 5. Carbonyl (a) and carboxyl (b) contents of OWSs at different catalyst concentrations and oxidation duration.

cm^{-1} band ratio seems to be a good indicator [42,43]. Slight variations were observed in this band area following the Fenton reaction prepared at higher catalyst concentration (above 0.4 wt %) or after 4 h duration. The main variation concerned the 1048 cm^{-1} band, which was found to have a reduced intensity for most OWSs. This could be related to the degradation of starch's crystalline structure due to the depolymerization of the macromolecular chain [34–37,44,45]. Because of the strong overlapping of the 1048, 1022 and 998 cm^{-1} bands, their evaluation remained challenging, and it was impossible to make safe conclusions.

3.2.2. *Determination of the level of oxidation: carbonyl and carboxyl titration*

Although the absorption peak at 1735 cm^{-1} confirmed the oxidation, the degree of oxidation could hardly be evaluated due to the limitation of the ATR FTIR analysis. In this configuration, penetration depth is typically a few micrometers, smaller than the typical starch granule diameter. This could lead to a measurement mostly of the starch granule surface and overestimating global starch oxidation. Instead, the various carbonyl and carboxyl contents of OWSs were used to quantify the oxidation extent. Both were determined following the titration methods present in Section 3.4. and shown in Fig. 5.

As expected, the carbonyl and carboxyl contents of OWSs increased rapidly with oxidation duration, confirming the formation of new chemical groups. The highest carbonyl and carboxyl contents of respectively 8.6 and 7 % were observed for the OWS at 1 wt % of catalyst after a 4 h process duration. After 4 h, the OWS prepared with 0.1 wt % of catalyst reached a maximum of its carboxyl content at 2 %. Its carbonyl content reached a maximum of 5.5 % after 6 h of treatment. After this point, the stabilization or fall of the carbonyl and carboxyl contents could be explained by the consumption of the oxidizing agent and by the scission of the starch macromolecule. Oxidation at the C2 and C3 positions is known to weaken the glucose unit by opening the monomeric ring, thus making the chains' depolymerization easier at those points [46]. As such, the extension of the Fenton reaction would only imply the degradation of the already oxidized chains. Similarly, the OWSs prepared with catalyst concentration between 0.2 and 0.5 wt % presented a rise of their carbonyl and carboxyl contents in the first 2 h of treatment, and a moderate one between 2 and 4/6 h when significant mass loss took place (Fig. 2). The addition of carbonyl/carboxyl is known to raise the starch reactivity [8–10,12,13], but comes at the cost of macromolecular and microstructural degradation [34–37,47]. For the targeted application of OWS in wood adhesives, it is desirable to obtain the most reactive starch possible for the lowest level of degradation and mass loss. As such, the impact of oxidation on the OWS structure and microstructure needs to be investigated in addition to the oxidation content.

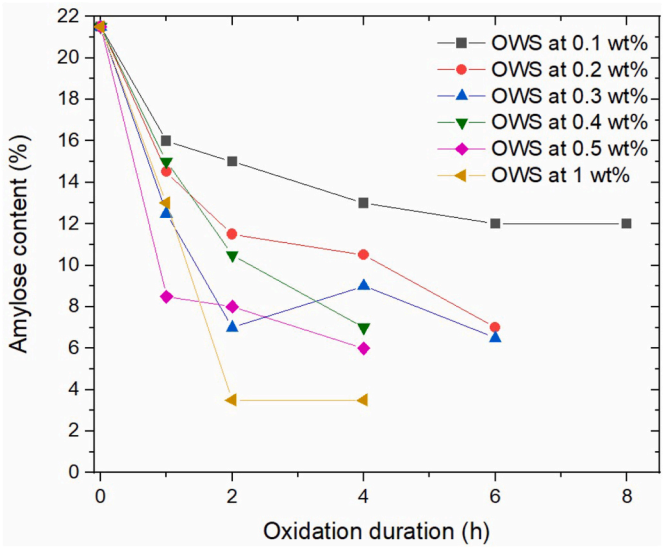

Fig. 6. Amylose content of the OWSs at different catalyst concentrations and oxidation duration.

3.3. *Effect of reaction conditions on starch microstructure, crystallinity, and structural properties*

The starch in this work was used without gelation and thus retained its granular shape. Starch granule architecture is formed by concentric growth rings [47], each ring is composed of semi-crystalline blocklets and amorphous rings. The blocklets' crystalline phase is mainly formed of the amylopectin linear segment, with its amorphous phase formed of the amylopectin branched point [47]. The amorphous rings are formed of amylose and some amylopectin macromolecular chains [47]. Due to this architecture, two parts of the starch structure are expected to be degraded in priority because of their presence in the amorphous phase, and thus easier to be penetrated by the oxidizing agent; the amylose [4,20,25,26,34], and the amylopectin branched point [4,5,17]. However the extent of degradation depends primarily on the starch origin and its characteristics, such as the initial amylose content, crystallinity level, and initial morphology [4,5,17].

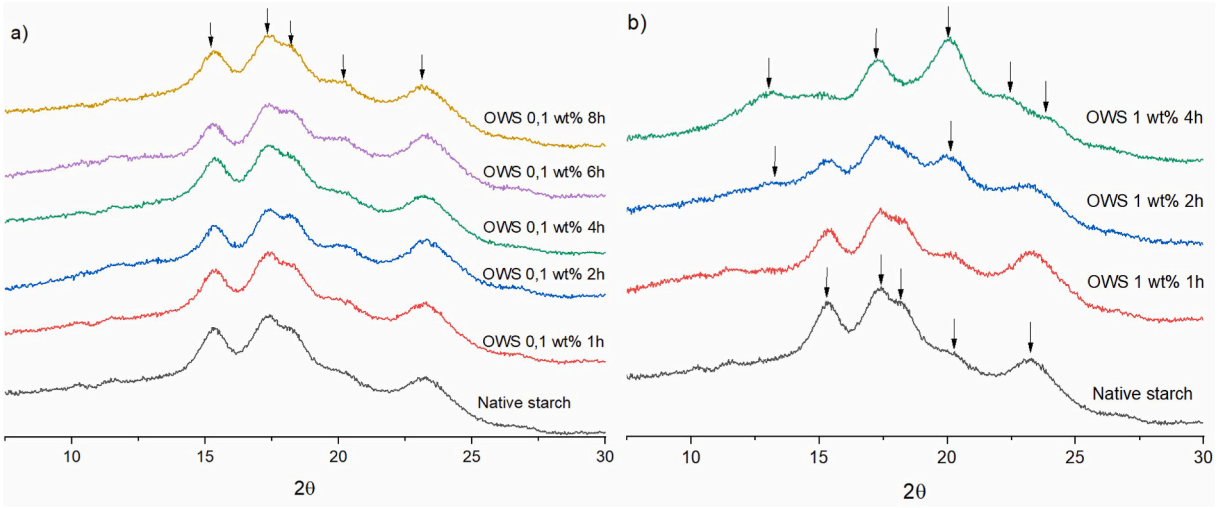

Fig. 7. Wide-angle X-ray diffraction patterns of OWSs prepared with 0.1 wt % (a) and 1 wt % (b) of catalyst and different oxidation duration.

3.3.1. *Effect on the reaction on the amorphous phase: amylose content determination*

To determine if the amylose and amylopectin were affected in the same proportion by the oxidation, the amylose content of OWSs was measured and presented in Fig. 6. The variation of amylose content in OWSs would indicate which of the two mechanisms mentioned before was predominant.

Native starch had an amylose content of 21.5 %, which is in accordance with the previously reported values for wheat starch [48,49]. For each catalyst concentration, an apparent reduction was observed in the amylose content as a function of the Fenton reaction with process duration. After 2 h, the OWS at 1 wt % of catalyst presented the lowest value with an amylose content below 4 %. This drastic reduction of amylose content of OWSs confirmed that the macromolecular degradation predominantly took place in the amorphous ring of the starch granule [6,15,50]. This type of degradation can significantly affect any polymer material's properties, with a reduction of the mechanical properties or even a complete loss of ductile behaviour [27,28]. Due to the targeted application of OWS in wood adhesives, this type of degradation must be avoided to the maximum extent.

3.3.2. *Effect of the reaction on the OWS crystalline phase: XRD diffraction*

In addition to the amorphous phase analysis by amylose content measurement, the crystalline structure of starch samples as a result of oxidation was analyzed with the XRD method. Figs. 7a and 6b illustrate the X-ray diffractograms of OWSs at 0.1 and 1.0 wt % of catalyst and different oxidation duration. The remaining diffractograms are present in supplementary files (Fig. S7).

Native (unmodified) starch showed an orthorhombic crystalline structure, a typical A-type starch diffraction pattern [50]. This crystalline structure is characterized by five diffraction peaks around 15, 17, 18, 20 and 23° [44]. No apparent changes were observed in the starch structure after oxidation with 0.1 wt % of catalyst. This is explained by the concentration of the reaction inside the amorphous part, as shown by changes in the amylose content, which kept the crystalline part mostly intact. A change of the diffraction peak position would have been linked to a change in the crystalline interplanar distance. For most catalyst concentration levels, the only change observed was the appearance of slightly sharper diffraction peaks than those in native starch samples. The crystalline structure of the OWS at 1 wt % of catalyst content (Fig. 6b) presented the most prominent change. For instance, OWS for 2 h showed two new peaks at 13 and 22°, and a lower relative intensity of peaks at 15, 17, and 18°. This reflects a substantial loss of A-type crystallinity in favour of an A + V-type structure. Such a mechanism was

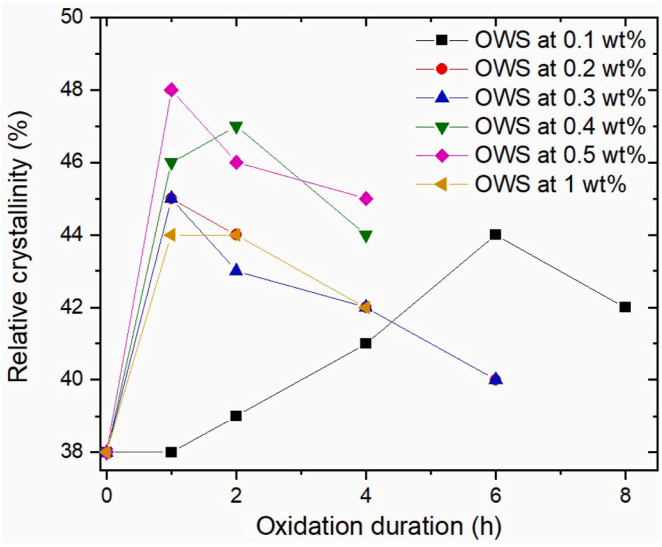

Fig. 8. Relative crystallinity (%) of OWSs as function of the catalyst concentration and process duration.

observed previously in other modified starches, e.g. starch extruded with fatty acid [44], after retrogradation [45] or acid complexes treatment [37], which is mainly related to the destruction of the double amylopectin helices that form the A-type crystalline structure, and is attributed to a high level of degradation.

The calculated relative crystallinity of OWSs at different catalyst levels and oxidation duration ranged from 38 % to 48 %, as presented in Fig. 8, while the unmodified starch showed a relative crystallinity estimate at 38 %. For each process duration, the relative crystallinity values of OWSs were found to increase up to a catalyst content of 0.5 wt % and then decrease when 1.0 wt % catalyst content was used. The apparent increase in crystallinity is explained by the degradation of the amorphous part previously confirmed by the amylose content determination [45]. The relative crystallinity was calculated by the area ratio between the crystalline diffraction peaks and the total spectra area (crystalline peaks and amorphous halo). The depolymerization of the amylose chains in the amorphous phase implied a reduction of the amorphous fraction in the starch structure and, as such, a diminution of the amorphous halo area. This resulted in a rise in the starch relative crystallinity.

Another mechanism is related to the degradation of starch inside the

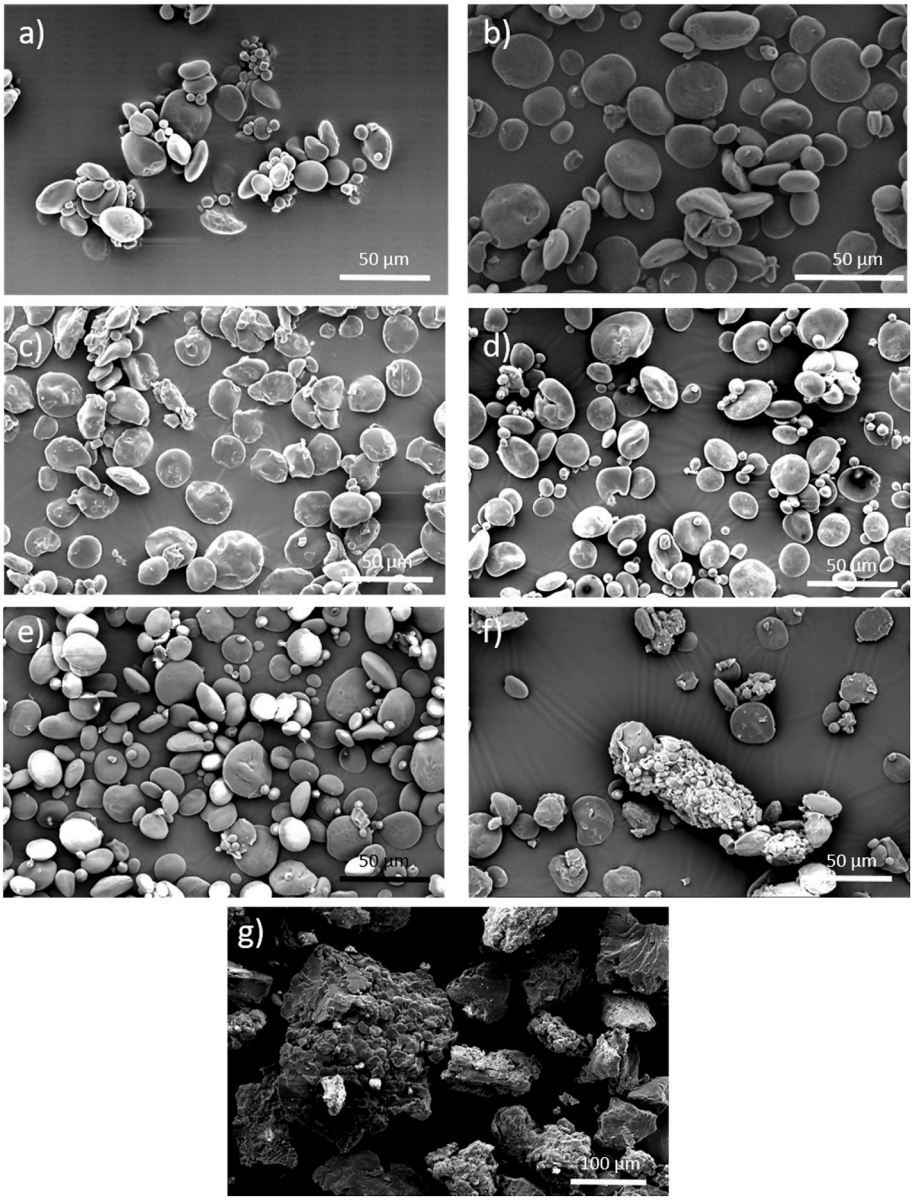

Fig. 9. SEM images of unmodified starch (a), and OWSs prepared with 0.3 wt % of catalyst for 4 h (b), 0.5 wt % of catalyst after 1 h (c) and, 2 h (d), and 1 wt % of catalyst after 1 h (e), 2 h (f) and 4 h (g).

amorphous phase, previously observed, due to depolymerization but also due to cleavage, which may create short amylose chain segments that can reorder and produce small crystalline segments or extend already existing crystalline lamella [51]. It results in a more defined crystalline structure and sharper diffraction peaks. This was observed for the OWSs prepared at low catalyst concentration and short oxidation duration. Similar behaviour was previously observed in oxidation reactions [4,6] or acid thinning [6,37,50] of starch. Except for the lowest catalyst concentration, prolonging the oxidation duration led to a reduction in relative crystallinity (Fig. 8). This could be attributed to the degradation of the crystalline structure of starch, although to a minor extent. Similar behavior was reported previously for the oxidation of corn, rice or potato starches by various levels of hypochlorite [4,15], and it was also confirmed by the vibration bands between 980 and 1100 cm^{-1} with FTIR spectroscopy (Fig. 3). Oxidation of starch at 1.0 wt % catalyst concentration caused critical degradation of starch macromolecules, as shown by the shifting of the crystallinity from A-type to A + V-type (Fig. 6b).

Both the degradation of the macromolecules in the amorphous phase and the degradation of the crystalline structure are problematic secondary effects of the oxidation reaction. For the scope of this study, an optimum oxidation level can be obtained with the OWS prepared with 0.1 wt % of catalyst and 4 h duration. Reaching a higher level of oxidation results in degradation of the amorphous phase first, then the crystalline phase, which would negatively affect the starch properties.

3.4. Effect of reaction conditions on starch morphology and granular shape

Observations under SEM were used to illustrate the changes in the morphological features of starch granules following the oxidation through the Fenton reaction (Fig. 9a–g). All SEM images displayed bimodal starch granules (large and small), which is characteristic of wheat starch. In general, the appearance of OWS granules resembled these of unmodified starch granules. A closer look showed that the smooth surfaces of native starch granules (Fig. 9a) were gradually changed into rough surfaces (Fig. 9b) with increasing catalyst concentration levels and oxidation duration. Regions of visible granule damage

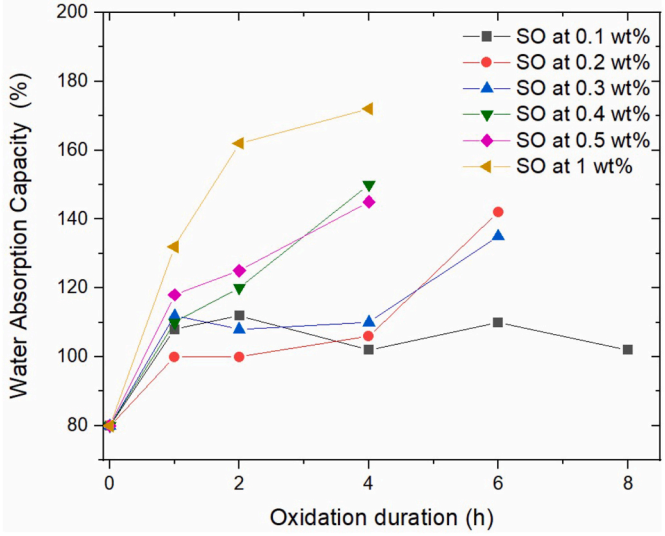

Fig. 10. WHC of the OWSs at different catalyst concentrations and oxidation duration.

were also evident. The most prominent change appeared at 0.5 and 1.0 wt % catalyst concentrations after 1 h of oxidation, while minor changes were detected at catalyst levels below 0.5 wt % (Fig. 9c and e). Extension of the oxidation to 2 h resulted in extensive degradation of the starch granules for the 0.5 wt % (Fig. 9d) and the formation of large agglomerates at 1 wt % (Fig. 9f). Similar surface alterations and damages of starch granules were reported previously after oxidation with hypochlorite [4,15,26,45]. As shown in the previous chapter, a longer oxidation process led to the degradation of the starch structure, shifting from A-type to A + V-starch type. As a result, the initial starch granule shape almost disappeared at 1 wt % of catalyst concentration and 4 h oxidation (Fig. 9g), forming a large agglomerate. Such a fragmentation verified that the oxidization reaction occurred not only on the surface of the starch granules but also within the structure. The formation of agglomerates, in addition to the degradation of the granule microstructure and morphology, implies a reduction of the starch available surface and, as such, the reactivity of OWS for future applications like the production of wood adhesives might be compromised. In addition, some of the carbonyl and carboxyl groups introduced by the Fenton reaction on the granules' surfaces would be trapped inside those agglomerates, thus reducing their availability for reactions.

3.5. Effect of reaction conditions on water absorption capacity (WAC)

The WAC values rapidly increased with reaction time for most catalyst concentration levels (Fig. 10). Native wheat starch had a WAC value of 85 %, which was slightly higher than the previously reported value of 58.9 % [52]. This might be related to the purity of samples and the granule architecture [52]. A reaction time of 1 h was sufficient for increasing the WAC of OWSs at 0.1 wt % catalyst to almost its maximum level, and then the WAC varied little. As expected, the highest values and steepest increase of WAC were obtained at 1 wt % catalyst level. The WAC of starch macromolecules is believed to be linked to their capability to form hydrogen bonds, and it is regulated by the crystalline structure of starch by the formation of longer double helices [53]. Thus, the reduction of amylose content due to the Fenton reaction increased the WAC of starch. Due to oxidation, the introduction of bulky carboxyl and carbonyl groups also causes electrostatic repulsion among starch molecules, thereby facilitating water access into the starch matrices [54]. The degradation of the amorphous phase and damage of starch granules following the oxidation create a more open structure that affects the starch ability to trap water [55].

3.6. Effect of reaction conditions on thermal stability

In order to be used in wood adhesive applications, the OWSs need to present thermal stability in the range of the temperature used for such applications, i.e. from 110 to 210 °C. The thermal stability of OWSs was evaluated through thermogravimetric (TG) and derivative thermogravimetric (DTG) analysis. For illustration, TG and DTG curves of OWS at various catalyst concentrations for a 4 h reaction are presented in Fig. 11. The remaining curves are presented in Supporting Information (Figs. S8–S12). The unmodified starch presented two mass losses, the first around 10 % at 100 °C, associated with the trapped moisture evaporation. The second one, around 300 °C, is associated with starch thermal degradation, with an onset temperature of 285 °C and a weight loss peak at 306 °C. The residual weight was around 20 %. All the OWSs prepared with a catalyst concentration between 0.1 and 0.4 wt % presented a similar thermal degradation behaviour with slight variations. For those starches, the second mass loss associated with the starch thermal degradation shifted to a lower temperature, with onset between 275 and 282 °C, and a weight loss peak between 295 and 302 °C.

This effect was even more visible for the OWSs prepared at 0.5 and 1 wt % catalyst levels. For both concentrations, OWSs after 1 and 2 h reaction time presented the same fall of their weight loss peak between 300 and 302 °C, and an onset at a much lower temperature under 260 °C. The main changes appeared after 4 h of oxidation, with their weight loss peak falling at 285 and 280 °C, respectively. An increase in

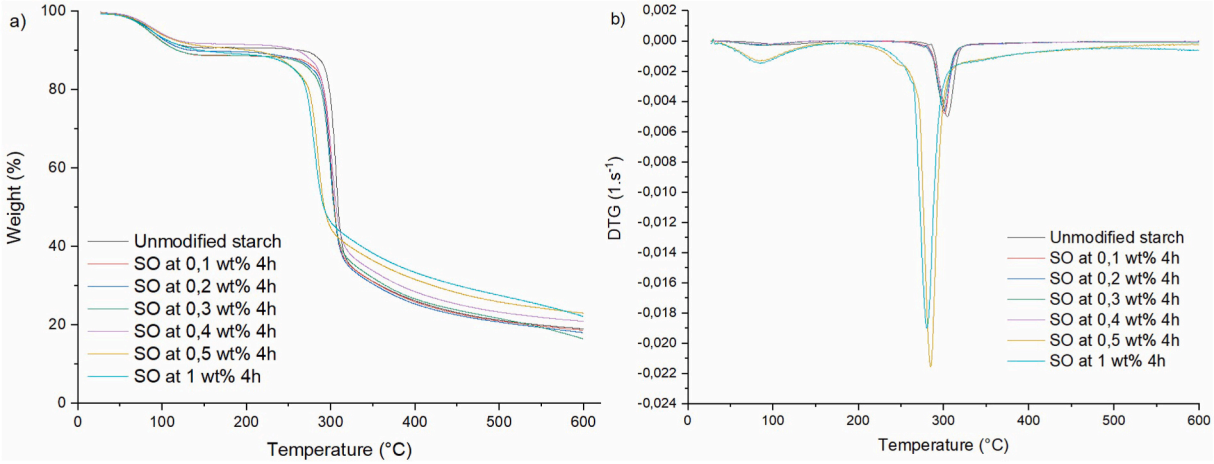

Fig. 11. Weight loss (a) and DTG (b) curves all OWSs prepared at various catalyst concentrations for 4 h oxidation duration.

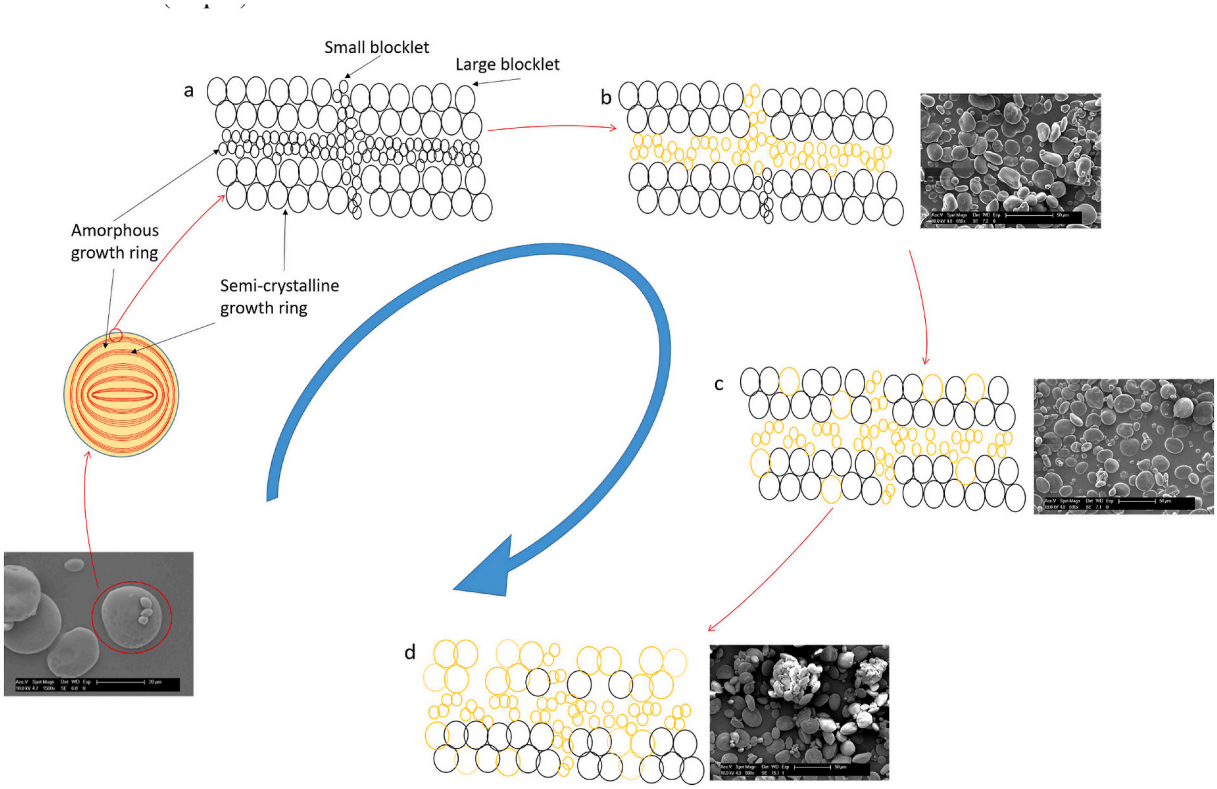

Fig. 12. Schematic overview of the evolution of starch oxidation steps: initial starch microstructure with amorphous and semi-crystalline ring (a), oxidation of the amorphous phase starting from le surface layers (b), propagation of the oxidation deeper in the amorphous phase, amorphous macromolecule degradation, beginning of the crystalline structure oxidation (c), and highly degraded microstructure and morphology, with aggregation of the granule (d).

the degree of oxidation leads to depolymerization of molecular chains, which causes a decrease in molecular weight and a subsequent decrease in the thermal stability of starch [46]. In addition, the highest number of carbonyl and carboxyl groups in the starch structure results in a higher reactivity and can imply an early degradation. The extensive degradation of the starch glucose groups and the degradation of the crystalline structure, from the A-type to the A + V type, had a pronounced impact on the thermal stability of OWSs. Interestingly, even the highly degraded OWS prepared at 1 wt % catalyst and 4 h duration still presented a thermal degradation temperature high enough to be used in the elaboration of wood adhesives. The lower thermal stability of the OWSs following the reaction could become a problem for producing wood adhesives when thermal-activated curing is used, like in the production of polyurethanes [8–10,12,13]. As such, the OWSs produced with a low catalyst concentration (<0.4 wt %) remained the most promising candidates.

3.7. Oxidation mechanism and implications for use of OWS in wood adhesives

The results provided a thorough understanding of the particular oxidation mechanism and the effect of Fenton reaction parameters on the structure, morphology and functional properties of OWSs. The reaction can be divided into various steps, as shown in Fig. 12. In its unmodified state, wheat starch presents a granule morphology with growth rings and a semi-crystalline structure (step a). When the oxidation reaction was initiated, the oxidation occurred mainly in the surface layers of the starch granules in the amorphous growth rings, which are composed mostly of amylose. In this step, the carbonyl and carboxyl contents of the starch increased rapidly to a level correlated to the catalyst concentration used (step b). Because of the low level of mass loss, absence of structural degradation, and the high concentration of highly reactive groups on the granule surface, making them easy to access and react with, these OWSs are promising for producing wood adhesives. As the oxidation progressed further, the already oxidized amylose chains in the amorphous phase began to be degraded by depolymerization and β-scission, resulting in a rise of starch relative crystallinity and stabilization of carbonyl and carboxyl contents. As a result, the starch granules were damaged, and their surfaces became rough. Even if a slightly higher oxidation level is obtained, it comes with a significant material loss. In addition, the groups produced inside the granules will not be readily available for reactions.

Further down in the oxidation process (step c), for example, with a reaction time of 4 h and above for most catalyst concentration levels, the semi-crystalline structure of starch granules was also degraded with a fall of relative crystallinity and a significant mass loss. This step further opened the granules' surface, allowing the oxidation to proceed in the inner layers. Finally, for harsher oxidation conditions with a catalyst concentration above 0.5 wt %, the starch macromolecules were degraded to such an extent that the classic A-type crystallinity was replaced by an A + V-type, and granule agglomerations were created (step d).

4. Conclusions

Wheat starch was oxidized by the Fenton reaction with the help of an Iron catalyst at various concentrations and oxidation durations. The formation of new chemical groups, mostly carbonyls and carboxyls, was evidenced by FTIR spectroscopy and chemical titration. The multiscale characterization of the OWSs gave insights into the reaction effect on the starch macromolecule, microstructure and morphology.

- At low catalyst concentration (≤0.3 wt %) or short oxidation duration (<4 h), the Fenton reaction was concentrated mainly in the amorphous ring of the starch granules. This resulted in

depolymerization of the amylose macromolecules in the amorphous phase and an opening of the granule surface.
- At higher catalyst concentrations (≥0.4 wt %) or long oxidation duration (>4 h), it became possible to reach a higher oxidation level at the cost of an important material loss resulting from the starch macromolecule depolymerization. In addition, the starch microstructure and morphology presented significant alternations and degradation of the crystalline lamellas.
- When the starch oxidation was extended enough, an agglomeration of the starch granules was observed. This is correlated to a switch of crystalline microstructure with the classic A-type starch crystalline structure changing to a more unusual A + V type, and the initial granule structure completely disappearing.

With those results, it became possible to produce OWS with the highest oxidation level possible and minimum mass loss, chain depolymerization, and change of microstructure and morphology. Such modified starch polymers present the advantages of concentrating oxide groups (carbonyl and carboxyl) on their granules' surfaces without degrading their structural, thermal, and physical properties. OWSs prepared with a catalyst concentration between 0.1 and 0.3 wt % are promising candidates for producing wood adhesives [8–10,12,13].

Funding

The authors acknowledge funding provided by Vinnova within the BioInnovation program for the project "Novel starch-based adhesive systems to enable recycling of fibreboards" (project number 2020–01918). A.L. also received funding by The Bridge, a strategic partnership between Linnaeus University, Södra and IKEA.

Institutional review board statement

Not applicable.

Informed consent statement

Not applicable.

CRediT authorship contribution statement

Adrien Letoffe: Writing – review & editing, Writing – original draft, Visualization, Methodology, Investigation, Formal analysis, Conceptualization. **Reza Hosseinpourpia:** Writing – review & editing, Validation, Methodology, Conceptualization. **Valentin Silveira:** Writing – review & editing, Methodology. **Stergios Adamopoulos:** Writing – review & editing, Validation, Resources, Funding acquisition, Conceptualization.

Declaration of competing interest

The authors declare that they have no known competing financial interests or personal relationships that could have appeared to influence the work reported in this paper.

Data availability

Data will be made available on request.

Acknowledgments

R.H. thanks the support of Formas (Future research leaders, Grant No. 2018–00637).

Appendix A. Supplementary data

Supplementary data to this article can be found online at https://doi.org/10.1016/j.carres.2024.109190.

References

[1] H. Li, S. Prakash, T.M. Nicholson, M.A. Fitzgeral, R.G. Gilbert, The importance of amylose and amylopectin fine structure for textural properties of cooked rice grains, Food Chem. 196 (2016) 702–711.
[2] A. Serrero, S. Trombotto, P. Cassagnau, Y. Bayon, P. Gravagna, S. Montanari, L. David, Polysaccharide gels based on chitosan and modified starch: structural characterization and linear viscoelastic behavior, Biomacromolecules 11 (2010) 1534–1543.
[3] M.M. Sánchez-Rivera, F.J.L. García-Suárez, M. Velázquez del Valle, F. Gutierrez-Meraz, L.A. Bello-Pérez, Partial characterization of banana starches oxidized by different levels of sodium hypochlorite, Carbohydrate Polym. 62 (1) (2005) 50–56.
[4] D. Kuakpetoon, Y. Wang, Structural characteristics and physicochemical properties of oxidized corn starches varying in amylose content, Carbohydr. Res. 341 (2006) 1896–1915.
[5] L.S. Matsuguma, L.G. Lacerda, E. Schnitzler, M.A. da Silva Carvalho Filho, C. M. Landi Franco, I.M. Demiate, Characterization of native and oxidized starches of two varieties of Peruvian carrot (arracacia xanthorrhiza, B.) from two production areas of paraná state, Brazil, Braz. Arch. Biol. Technol. 52 (2009) 701–713.
[6] O.S. Lawal, K.O. Adebowale, B.M. Ogunsanwo, L.L. Barba, N.S. Ilo, Oxidized and acid thinned starch derivatives of hybrid maize: functional characteristics, wide-angle X-ray diffractometry and thermal properties, Int. J. Biol. Macromol. 35 (2005) 71–79.
[7] I. Hanafi, I. Maryam, A. Zulkifli, Starch-based hydrogels: present status and applications, International Journal of Polymeric Materials and Polymeric Biomaterials 62 (2013) 411–442.
[8] R. Hosseinpourpia, A. Eceiza, S. Adamopoulos, Polyurethane wood adhesives prepared from modified polysaccharides, Polymers 14 (3) (2022) 539.
[9] N. Neitzel, R. Hosseinpourpia, S. Adamopoulos, A dialdehyde starch-based adhesive for medium-density fiberboards, Bioresources 18 (1) (2023) 2155–2171.
[10] R. Hosseinpourpia, S. Adamopoulos, C. Mai, H.R. Taghiyari, Properties of medium-density fibreboards bonded with dextrin-based wood adhesive, Wood Res. 64 (2) (2019) 185–194.
[11] K. Neelam, S. Vijay, S. Lalit, Various techniques for the modification of starch and the application of its derivatives, Int. Res. J. Pharm. 3 (5) (2012) 25–31.
[12] R. Hosseinpourpia, A.S. Echart, S. Adamopoulos, N. Gabilondo, A. Eceiza, Modification of pea starch and dextrin polymers with isocyanate functional groups, Polymers 10 (9) (2018) 939.
[13] R. Hosseinpourpia, S. Adamopoulos, A.S. Echart, A. Eceiza, Polyurethane films prepared with isophorone diisocyanate functionalized wheat starch, Eur. Polym. J. 161 (2021) 110826.
[14] N. Masina, Y.E. Choonara, P. Kumar, L.C. du Toit, M. Govender, S. Indermun, V. Pillay, A review of the chemical modification techniques of starch, Carbohydr. Polym. 157 (2017) 1226–1236.
[15] D. Kuakpetoon, Y. Wang, Characterization of different starches oxidized by hypochlorite, Starch Staerke 53 (2001) 211–218.
[16] R. Tang, Y. Du, L. Fan, Dialdehyde starch-crosslinked chitosan films and their antimicrobial effects. Journal of polymer science: Part B, Polymer Physics 41 (2003) 993–997.
[17] K. Lewicka, P. Siemion, P. Kurcok, Chemical modifications of starch: microwave effect, International Journal of Polymer Science 2015 (2015) 1–10.
[18] P. Tomasik, C.H. Schilling, Chemical modification of starch, Adv. Carbohydr. Chem. Biochem. 59 (2004) 175–403.
[19] R.J. Hugh, Non degradative reactions of starch, in: R.L. Whistler, E.F. Paschall (Eds.), Starch Chemistry and Technology vol. I, Academic Press, New York, 1965, pp. 430–487.
[20] H. Isbell, H. Frush, Mechanisms for hydroperoxide degradation of disaccharides and related compounds, Carbohydr. Res. 161 (2) (1987) 181–193.
[21] P. Tolvanen, A. Sorokin, P. Mäki-Arvela, S. Leveneur, D. Murzin, T. Salmi, Batch and semibatch partial oxidation of starch by hydrogen peroxide in the presence of an iron tetrasulfophthalocyanine catalyst: the effect of ultrasound and the catalyst addition policy, Ind. Eng. Chem. Res. 50 (2011) 749–757.
[22] R.E. Harmon, S.K. Gupta, L. Johnson, Oxidation of starch by hydrogen peroxide in the presence of UV light-Part II, Starch 24 (1) (1972) 8–11.
[23] N. Vatanasuchart, O. Naivikul, S. Charoenrein, K. Sriroth, Molecular properties of cassava starch modified with different UV irradiations to enhance baking expansion, Carbohydr. Polym. 61 (2005) 80–87.
[24] J. Kuntail, S. Pal, I. Sinha, Interfacial phenomena during Fenton reaction on starch stabilized magnetite nanoparticles: molecular dynamics and experimental investigations, J. Mol. Liq. 318 (15) (2020) 114037.
[25] S. Pietrzyk, T. Fortuna, Oxidation-induced changes in the surface structure of starch granules, Pol. J. Food Nutr. Sci. 14/55 (2) (2005) 159–164.
[26] K. Sangseethong, N. Termvejsayanon, K. Sriroth, Characterization of physicochemical properties of hypochlorite and peroxide-oxidized cassava starches, Carbohydr. Polym. 82 (2010) 446–453.
[27] Y. Minoura, M. Ueda, S. Mizunuma, M. Oba, The reaction of polypropylene with maleic anhydride, J. Appl. Polym. Sci. 13 (1969) 1625–1640.

[28] R. Zhang, Y. Zhu, J. Zhang, W. Jiang, J. Yin, Effect of the initial maleic anhydride content on the grafting of maleic anhydride onto isotactic polypropylene, Journal of Polymer Science: Part A: Polymer Chemistry 43 (2005) 5529–5534.
[29] Y. Zhang, L. Ding, J. Gu, H. Tan, L. Zhu, Preparation and properties of a starch-based wood adhesive with high bonding strength and water resistance, Carbohydr. Polym. 115 (2) (2015) 32–37.
[30] M.K. Chapagai, B. Fletcher, T. Witt, S. Dhital, B.M. Flanagan, M.J. Gidley, Multiple length scale structure-property relationships of wheat starch oxidized by sodium hypochlorite or hydrogen peroxide, Carbohydrate Polymer Technologies and Applications 2 (2021) 100147.
[31] P.S. Landers, E.E. Gbur, R.N. Sharp, Comparison of two methods to predict amylose concentration in rice flours as determined by spectrophotometric assay, Cereal Chem. 68 (5) (1991) 545–548.
[32] T. Zhu, D.S. Jackson, R.L. Wehling, B. Geera, Comparison of amylose determination methods and the development of a dual wavelength iodine binding technique, Cereal Chem. 85 (2008) 51–58.
[33] M. Kačuráková, M. Mathlouthi, FTIR and laser-Raman spectra of oligosaccharides in water: characterization of the glycosidic bond, Carbohydr. Res. 284 (2) (1996) 145–157.
[34] Q. Zhu, E. Bertoft, Enzymic analysis of the structure of oxidized potato starches, Int. J. Biol. Macromol. 21 (1997) 131–135.
[35] M.W. Rutenberg, D. Solarek, Starch derivatives: productionand uses, in: R. L. Whistler, J.N. BeMiller, E.F. Paschall (Eds.), Starch: Chemistry and Technology, second ed., Academic Press, New York, 1984.
[36] N.L. Vanier, S.L.M. El Halal, A.R.G. Dias, Zavareze E. da Rosa, Molecular structure, functionality and applications of oxidized starches: a review, Food Chem. 221 (2017) 1546–1559.
[37] S. Meng, Y. Ma, D.W. Sun, L. Wang, T. Liu, Properties of starch-palmitic acid complexes prepared by high pressure homogenization, J. Cereal. Sci. 59 (1) (2014) 25–32.
[38] A. Para, Complexation of metal ions with dioxime of dialdehyde starch, Carbohydrate Polym. 57 (2004) 277–283.
[39] D.K. Kweon, J.K. Choi, E.K. Kim, S.T. Lim, Adsorption of divalent metal ions by succinylated and oxidized corn starches, Carbohydr. Polym. 46 (2) (2001) 171–177.
[40] F. Luo, Q. Huang, X. Fu, L. Zhang, S. Yu, Preparation and characterisation of crosslinked waxy potato starch, Food Chem. 115 (2) (2009) 563–568.
[41] M. Emeje, R. Kalita, C. Isimi, A. Buragohain, O. Kunle, S. Ofoefule, Synthesis, physicochemical characterization and functional properties of an esterified starch from an underutilized source in Nigeria, Afr. J. Food Nutr. Sci. 12 (2012) 7001–7018.
[42] K. Lizuka, T. Aishima, Starch gelation process observed by FT-IR/ATR spectrometry with multivariate data analysis, J. Food Sci. 64 (4) (1999) 653–658.
[43] P. Rubens, J. Snauwaert, K. Heremans, R. Stute, In situ observation of pressure-induced gelation of starches studied with FTIR in the diamond anvil cell, Carbohydr. Polym. 39 (3) (1999) 231–235.
[44] J.E. Cervantes-Ramírez, A.H. Cabrera-Ramirez, E. Morales-Sánchez, M. E. Rodriguez-García, M.L. Reyes-Vega, A.K. Ramírez-Jiménez, B.L. Contreras-Jiménez, M. Gaytán-Martínez, Amylose-lipid complex formation from extruded maize starch mixed with fatty acids, Carbohydr. Polym. 246 (2020) 116555.
[45] W. Li, X. Tian, P. Wang, A.S.M. Saleh, Q. Luo, J. Zheng, S. Ouyang, G. Zhang, Recrystallization characteristics of high hydrostatic pressure gelatinized normal and waxy corn starch, Int. J. Biol. Macromol. 83 (2016) 171–177.
[46] Y.R. Zhang, X.L. Wang, G.M. Zhao, Y.Z. Wang, Preparation and properties of oxidized starch with high degree of oxidation, Carbohydrate Polym. 87 (2012) 2554–2562.
[47] S. Naguleswaran, T. Vasanthan, R. Hoover, L. Chen, D. Bressler, Molecular characterisation of waxy corn and barley starches in different solvent systems as revealed by MALLS, Food Chem. 152 (2014) 297–299.
[48] J. Jane, Y.Y. Chen, L.F. Lee, A.E. McPherson, K.S. Wong, M. Radosavljevic, T. Kasemsuwan, Effects of amylopectin branch chain length and amylose contenton the gelatinization and pasting properties of starch, American Association of Cereal Chemists 76 (5) (1999) 629.
[49] J. Blazek, H. Salman, A.L. Rubio, E. Gilbert, T. Hanley, L. Copeland, Structural characterization of wheat starch granules differing in amylose content and functional characteristics, Carbohydr. Polym. 75 (2009) 705–711.
[50] C.E. Chávez-Murillo, Y. Wang, L.A. Bello-Pérez, Morphological, physicochemical and structural characteristics of oxidized barley and corn starches, Starch 60 (11) (2008) 634–645.
[51] L. Wang, Y. Wang, Structures and physicochemical properties of acid-thinned corn, Potato and Rice Starches 53 (11) (2001) 570–576.
[52] M. Schirmer, A. Höchstötter, M. Jekle, E. Arendt, T. Becker, Physicochemical and morphological characterization of different starches with variable amylose/amylopectin ratio, Food Hydrocolloids 32 (2013) 52–63.
[53] T. Sasaki, J. Matsuki, Effect of wheat starch structure on swelling power, Cereal Chem. 75 (1998) 525–529.
[54] O.S. Lawal, K.O. Adebowale, Physicochemical characteristics and thermal properties of chemically modified jack bean (*Canavalia ensiformis*) starch, Carbohydr. Polym. 60 (3) (2005) 331–341.
[55] K.O. Falade, C.A. Okafor, Physicochemical properties of five cocoyam (*Colocasia esculenta and Xanthosoma sagittifolium*) starches, Food Hydrocolloids 30 (1) (2013) 173–181.